

# Normal Patterns on $^{99m}\text{Tc}$ -ECD Brain SPECT Scans in Adults

Fumiko Tanaka, Douglass Vines, Tatsuro Tsuchida, Morris Freedman, and Masanori Ichise

*Division of Nuclear Medicine, Department of Medical Imaging, University of Toronto, Toronto; Division of Neurology, The Hospital for Sick Children, Toronto; Behavioural Neurology Program and Rotman Research Institute, Baycrest Center for Geriatric Care, Toronto; and Division of Neurology, Department of Medicine, Mount Sinai Hospital and University Health Network, Toronto, Ontario, Canada*

Normative ethyl cysteinyl dimer (ECD) SPECT data must be available to successfully apply ECD SPECT to clinical studies. The purpose of this study was to determine ECD SPECT scan patterns of healthy adults. **Methods:** Forty-eight healthy volunteers (22 men, 26 women; age range, 22–95 y; mean age,  $47.6 \pm 19.2$  y) underwent high-resolution ECD SPECT. For visual analysis of regional brain ECD uptake, we used a scale of +3 to -3, in which +3 and -3 indicated highest ECD uptake and deficit, respectively. For quantitative analysis, we measured the region-to-cerebellum ratio (R/CE) and the region-to-cerebral cortex ratio (R/CO) for 17 regions (13 cortical, 3 subcortical, and 1 cerebellar). **Results:** On visual analysis, no subject had a score of -3. All subjects had a score of -2 for the hippocampus and a score of +3 for the medial occipital cortex, except for 2 subjects who had a score of +3 for the striatum and thalamus. A frontal eye field and posterior parieto-occipital junction were identified in 60% of subjects with a score of +1 and 79% of subjects with a score of +2. On quantitative analysis, a significant regional variation (ANOVA,  $P < 0.0001$ ) was seen in R/CE, ranging from 0.709 (hippocampus) to 1.26 (medial occipital cortex). However, regional right-to-left differences and intersubject variability of R/CE were small (asymmetry index,  $3.6\% \pm 0.8\%$ ; coefficient variation,  $6.6\% \pm 0.7\%$ ). R/CE declined significantly with age in 6 regions, including the anterior and posterior cingulate cortex, superior prefrontal and parietal cortex, striatum, and hippocampus (1.0%–2.0% per decade,  $P < 0.05$ ), whereas R/CO in the cerebellum increased significantly with age (1.0% per decade,  $P < 0.05$ ). **Conclusion:** Although regional ECD brain perfusion patterns vary significantly, including variability caused by the age-related effect, intersubject variability is small. Recognition of these normal patterns is important for clinical interpretation of ECD SPECT studies.

**Key Words:**  $^{99m}\text{Tc}$ -ECD; brain SPECT; cerebral blood flow; normal patterns; aging

**J Nucl Med 2000; 41:1456–1464**

**A**s a clinical tool for evaluating regional cerebral blood flow (rCBF),  $^{99m}\text{Tc}$ -ethyl cysteinyl dimer (ECD) SPECT is widely used. It has several favorable characteristics (1–6), such as in vitro chemical stability lasting several hours after

reconstitution, fast blood clearance, and high signal-to-noise ratio. ECD SPECT studies show that this technique is useful for elucidating brain function impairment noninvasively and cost-effectively for various neurologic disorders, such as cerebrovascular disease (7–10), traumatic brain injury, epilepsy (11–12), Alzheimer's disease (13–15), and Parkinson's disease (16).

One factor critical to the successful application of ECD SPECT to clinical studies is the availability of ECD SPECT data for healthy individuals. Several lines of evidence suggest considerable normal variation in rCBF. First, rCBF variation may occur both within and between subjects (17). Loessner et al. (18) reported normal variations in regional metabolic activity using FDG PET. Specifically, they observed a frontal pole defect in 84%, a frontal eye field in 84%, and a posterior parieto-occipital junction in 58% of 120 healthy volunteers. These specific metabolic variations are expected to be detectable using rCBF SPECT because rCBF and regional glucose metabolism are usually coupled (19). Second, age affects cerebral circulation. PET studies have shown an age-related decline in gray matter rCBF to be regionally dependent (20–22). Third, some limitations of ECD as an rCBF imaging tracer have been reported. In particular, ECD SPECT underestimates rCBF in the high flow range (23), shows decreased ECD uptake in areas with luxury perfusion (7,24), and exhibits a regional clearance that varies from that in normal brain (25). Finally, comparative studies between ECD and other flow tracers, such as  $^{99m}\text{Tc}$ -D,L-hexamethyl propyleneamine oxime, have found some other characteristic ECD perfusion patterns in the brain. These studies have reported relatively low ECD uptake in the medial temporal region (26–28) and high ECD uptake in the medial occipital region (28,29) even if subjects were resting with their eyes closed at the time of ECD injection. These characteristic ECD perfusion patterns reflect the retention mechanism, which may be related to in vivo metabolism of ECD in the brain (1–2). However, the exact mechanism underlying these patterns remains unknown.

Recognition of rCBF patterns unique to ECD, as well as ECD perfusion patterns that reflect normal variation in

Received Oct. 4, 1999; revision accepted Feb. 2, 2000.

For correspondence or reprints contact: Fumiko Tanaka, MD, PhD, Rm. 635, Division of Nuclear Medicine, Mount Sinai Hospital, 600 University Ave., Toronto, Ontario, M5G 1X5 Canada.

rCBF, is imperative for the accurate interpretation of clinical ECD SPECT studies. To evaluate normal patterns in ECD SPECT scans, we studied 48 healthy adults with a wide age range (22–95 y) and evaluated normal variations in ECD perfusion patterns including those specific variations reported for FDG PET and those caused by age effects.

## MATERIALS AND METHODS

### Subjects

Forty-eight healthy volunteers (22 men, 26 women; age range, 22–95 y; mean age,  $47.6 \pm 19.2$  y) were studied. On the basis of a screening interview, none had a current or previous medical history that would influence the ECD study. None were taking medication. Eighteen were older than 50 y. All had normal Mini-Mental State Examination scores and normal MRI or CT findings. The study was approved by the institutional human subjects review committees. All subjects gave written informed consent.

### SPECT

The manufacturer's instructions were followed for preparation and quality control of the ECD. The subjects received injections of 740 MBq (20 mCi) ECD in a quiet room with their eyes open and their ears unplugged. SPECT was performed using a triple-head system (Prism 3000; Picker International, Inc., Cleveland, OH) equipped with ultra-high-resolution fanbeam collimators and interfaced to a dedicated computer. Image acquisition started 23–62 min after tracer injection. Data were collected for 40 views per camera head in a  $128 \times 128$  matrix. The radius of rotation was fixed at 13.5 cm. Acquired data were reconstructed using a 3-dimensional Butterworth filter (order, 6.0; cutoff frequency, 0.3 cycle per pixel) after applying a ramp backprojection filter.

### Image Data Analysis

We used our previously reported fully automated stereotactic image orientation program (30) to obtain 3 sets of gridded and nongrided tomographic images (transaxial, sagittal, and coronal

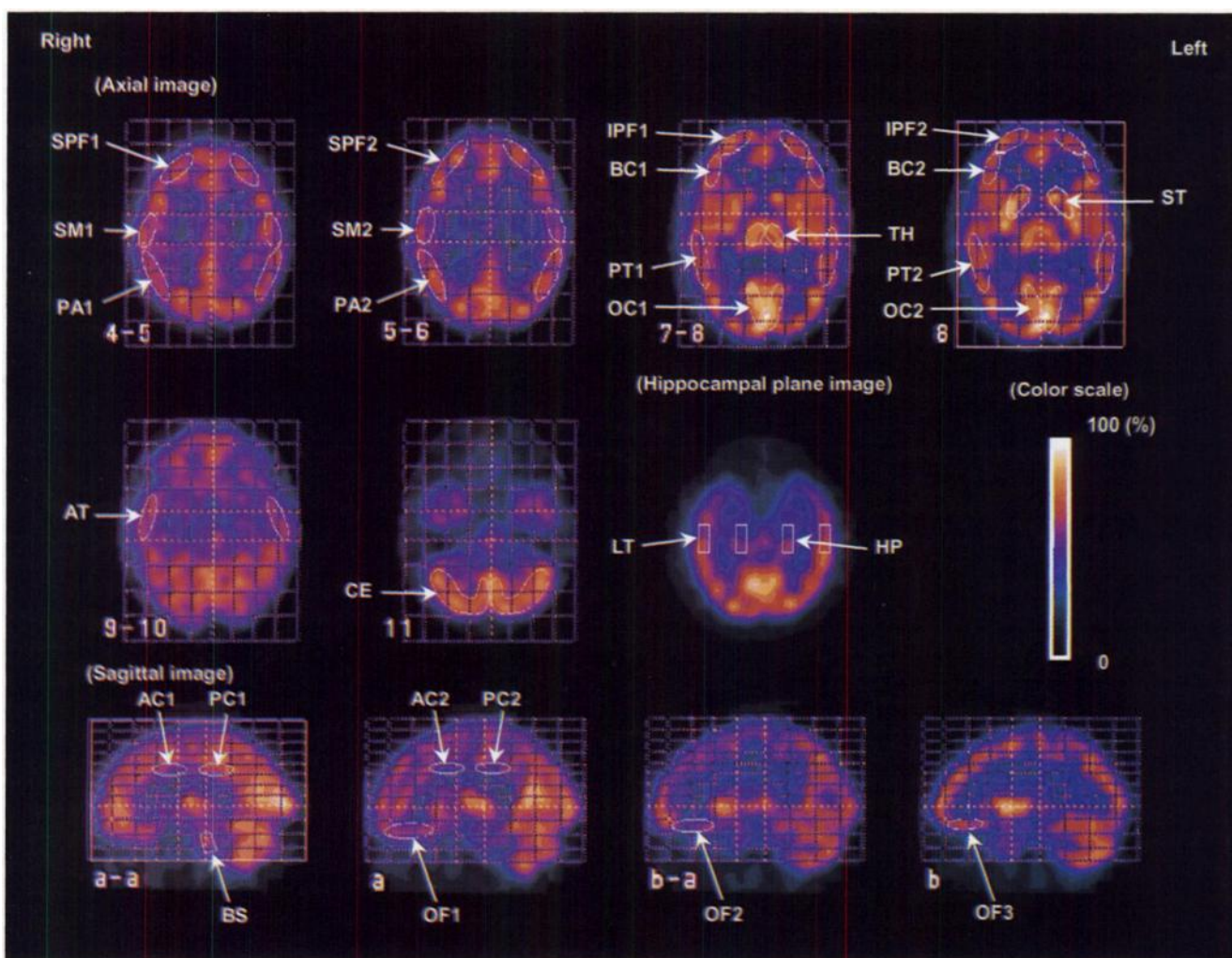


**FIGURE 1.** Region-of-interest templates placed on selected axial, hippocampal, and sagittal images. Slice numbers and letters correspond to those of Talairach et al. (31). Hippocampal image was manually reformatted along long axis of temporal lobe. AC (AC1, AC2) = anterior cingulate cortex; AT = anterior temporal cortex; BC (BC1, BC2) = Broca's area; BS = brain stem; CE = cerebellum; HP = medial temporal region including hippocampus; IPF (IPF1, IPF2) = inferior prefrontal cortex; LT = lateral temporal cortex; OC (OC1, OC2) = medial occipital cortex; OF (OF1, OF2, OF3) = orbitofrontal cortex; PA (PA1, PA2) = parietal cortex; PC (PC1, PC2) = posterior cingulate cortex; PT (PT1, PT2) = posterior temporal cortex; SM (SM1, SM2) = sensorimotor cortex; SPF (SPF1, SPF2) = superior prefrontal cortex; ST = striatum; TH = thalamus.

**TABLE 1**  
Visual Assessment of ECD Perfusion Patterns

ECD uptake	Score	Region	No. of subjects
Highest uptake of ECD	+3	Medial occipital cortex	44 (91.7%)
		Medial occipital cortex and frontal cortex	1 (2.1%)
		Medial occipital cortex and thalamus	2 (4.2%)
		Striatum	1 (2.1%)
Lowest uptake of ECD	-2	Medial temporal region including hippocampus	48 (100%)

sections) corresponding to the slices in the system of Talairach et al. (31). The images were displayed on a computer monitor using a cool color scale (window, 100; base, 0).

Both visual and quantitative image analyses were performed. For visual analysis, 3 nuclear medicine physicians with extensive brain SPECT experience interpreted the SPECT images and reached a consensus. No training for visual interpretation took place. We used a 7-grade rating scale that ranged from -3 to +3, in which -3 was a deficit; -2 and -1 were moderately and mildly low ECD uptake, respectively; 0 was baseline; +1 and +2 were mildly and moderately high ECD uptake, respectively; and +3 was the highest ECD uptake. A deficit was defined as a clear disconnection in brain ECD uptake in more than 3 continuous slices. For the quantitative analysis, 3 transverse images were manually selected (the best-visualized slices for basal ganglia, thalamus, and cerebellum), and an additional 10 images were automatically selected

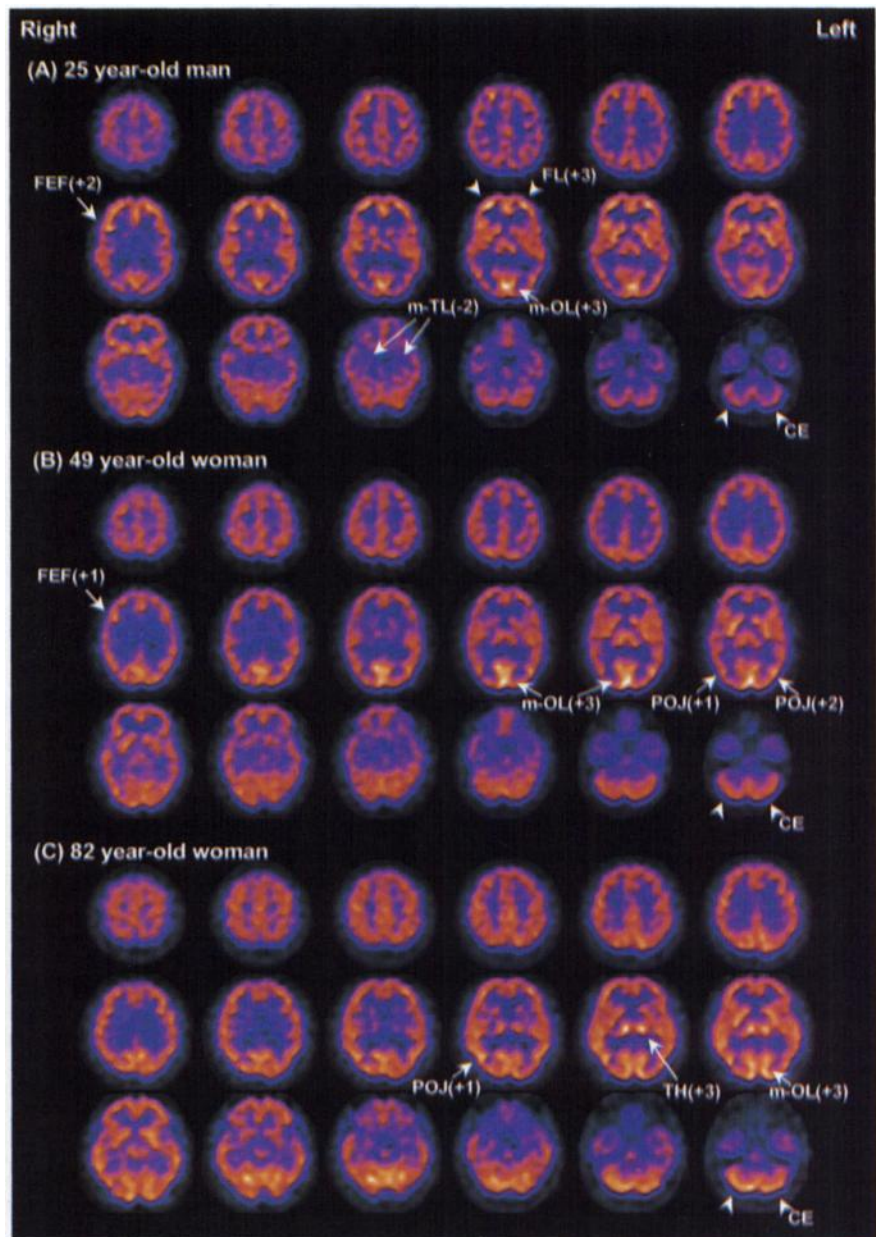


**FIGURE 2.** Selected transaxial ECD SPECT images of 3 healthy volunteers: 25-y-old man (A), 49-y-old woman (B), and 82-y-old woman (C). Highest ECD uptake, +3, was observed in medial occipital (m-OL) and frontal (FL) cortex in (A), m-OL in (B), and m-OL and thalamus (TH) in (C). Least ECD uptake, -2, was seen in medial temporal cortex (m-TL) in all subjects. Cerebellar (CE) ECD uptake increased with increasing age. Frontal eye field (FEF) and posterior parieto-occipital junction (POJ) were identified as focally increased ECD uptake in posterior frontal region and junction of parietal and occipital lobes, respectively. Numbers in parentheses are ECD uptake scores.

using a macroprogram. The transverse set included slices 4–5, 5–6, 7–8, 8, 9–10, and 11 and the sagittal set included slices a-a, bilateral a, a-b, and b, with slice numbers and letters corresponding to those in the system of Talairach et al. (31). Additionally, we manually resliced reconstructed images parallel to the long axis of the temporal lobe (hippocampal plane image) and selected the slice that best showed the hippocampus (Fig. 1). We measured ECD uptake in a total of 25 paired regions of interest (ROI) in both the left and the right hemispheres and 3 unpaired ROI templates on a midsagittal image (a-a) (Fig. 1). These ROIs ranged in volume from 2.0 cm<sup>3</sup> (brain stem) to 12.5 cm<sup>3</sup> (cerebellum) and were fixed in size across studies. ROI placement depended on visual identification of anatomic regions by stereotactic grid guidance. All ROIs were placed by the same operator to eliminate interoperator variability. The average coefficient of intraoperator variation in the quantitative measurements was 0.81% ± 0.56% (n = 10 times). To quantify regional ECD uptake, the mean counts in each selected region were normalized with respect to the mean counts in the cerebellum (region-to-cerebellum ratio [R/CE]) and in the cerebral cortex (region-to-cerebral cortex ratio [R/CO]). The mean counts in the cerebral cortex were obtained by averaging the counts in all ROIs in the cerebral cortex, excluding the anterior and posterior cingulate cortex, and in the hippocampus. The following 17 regions were defined individually or in combination, with slice numbers and letters corresponding to those in the system of Talairach et al. (31) (Fig. 1): superior prefrontal cortex (SPF1, SPF2); inferior prefrontal cortex (IPF1, IPF2); sensorimotor cortex (SM1, SM2); Broca's area (BC1, BC2); orbitofrontal cortex (OF1, OF2, OF3); parietal cortex (PA1, PA2); anterior temporal cortex; posterior temporal cortex (PT1, PT2); lateral temporal cortex; medial temporal region, including the hippocampus; medial occipital cortex (OC1, OC2); anterior cingulate cortex (AC1, AC2); posterior cingulate cortex (PC1, PC2); striatum; thalamus; brain stem; and cerebellum. AC1, PC1, and the brain stem were localized on the midsagittal plane (a-a).

### Statistical Analysis

An asymmetry index was calculated for all regions except the anterior cingulate cortex, posterior cingulate cortex, and brain stem using the following equation: asymmetry index = 2 × (R - L) / (R + L), where R is right and L is left. An unpaired *t* test was used

to evaluate the sex differences in regional ECD uptake. ANOVA was used to evaluate the differences in ECD uptake ratio (R/CE and R/CO) between hemispheres and regions. A posthoc Scheffé test was used to correct for multiple comparisons. The relationships between ECD uptake ratios and age were established using linear regression analysis. Statistical analyses were performed with STATISTICA (StatSoft, Inc., Tulsa, OK) software. Statistical significance was defined as *P* < 0.05.

## RESULTS

### Visual Analysis

The technical quality of the ECD SPECT images was excellent for 22 subjects (45.8%), good for 20 subjects (41.7%), and fair for 6 subjects (12.5%). In the visual scoring of ECD uptake, at least 1 rater disagreed about 4 patients (8.3%) for the cingulate cortex, 3 patients (6.3%) for the frontal eye field, and 3 patients (6.3%) for the parieto-occipital junction. Otherwise, the 3 raters agreed. No focal deficits with a score of -3 were reported for any subject. Thus, no frontal pole defect was identified. The highest ECD uptake, a score of +3, was reported for the medial occipital cortex of all subjects except 1, whose images were scored +3 for the striatum and +2 for the medial occipital cortex. The frontal cortex of 1 subject and the thalamus of 2 subjects were scored as +3, as was the medial occipital cortex (Table 1). The least ECD uptake, a score of -2, was recorded for the medial temporal region of all subjects (Fig. 2). The cingulate cortex received scores ranging from -1 to +1 (Fig. 3): a score of -1 for 13 subjects (27.1%), 0 for 27 subjects (56.3%), and +1 for 8 subjects (16.7%). The cerebellum showed a tendency toward increased ECD uptake relative to the cortex with increasing age (Fig. 2). Table 2 summarizes visual assessment of frontal eye fields and parieto-occipital junctions. These regions had scores of +1 or +2. A frontal eye field was seen in 29 subjects (60.4%), unilaterally in 15 (on the right in 9 [18.8%] and on the left in 6 [12.5%]) and bilaterally in 14 (29.2%). Bilateral frontal eye fields were symmetric in 10 subjects (20.8%),

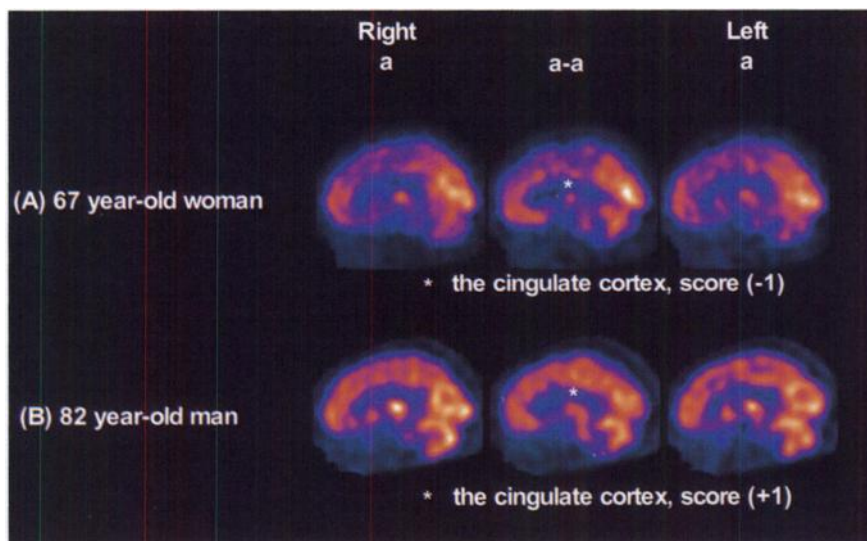


**FIGURE 3.** Sagittal images (slices a-a and a bilaterally, using the system of Talairach et al. (31)) of 2 healthy volunteers: 67-y-old woman (A) and 82-y-old man (B). Cingulate cortex showed variable ECD uptake ranging from -1 in (A) to +1 in (B).

**TABLE 2**  
Visual Assessment of FEF and POJ

Variation type	ECD uptake			Bilaterality		Unilaterality	
	Score	Right	Left	Present	With equal intensity	Right	Left
FEF	+1 or +2	23 (47.9%)	20 (41.7%)	14 (29.2%)	10 (20.8%)	9 (18.8%)	6 (12.5%)
POJ	+1 or +2	20 (62.5%)	28 (60.4%)	20 (41.7%)	14 (29.2%)	10 (20.8%)	8 (16.7%)

FEF = frontal eye field; POJ = posterior parieto-occipital junction.

with a score of +1 in 8 (16.7%) and a score of +2 in 2 (4.2%). A parieto-occipital junction was seen in 38 subjects (79.2%), unilaterally in 18 (on the right in 10 [20.8%] and on the left in 8 [16.7%]) and bilaterally in 20 (41.7%). Bilateral parieto-occipital junctions were symmetric in 14 subjects (29.2%), with a score of +1 in 12 (25.0%) and a score of +2 in 2 (4.2%). When the frontal eye field and parieto-occipital junction were unilateral, they were more often noted on the right than on the left.

#### Quantitative Analysis

The mean total brain ECD count 30 min after ECD injection was  $7.95 \pm 2.21$  million counts (range, 4.63–14.70 million counts). Regional ECD uptake ratios are summarized in Table 3 and shown in Figure 4. Using R/CE and R/CO, a significant regional difference ( $P < 0.0001$ ) was observed. The mean values of right and left R/CEs ranged from 0.709 (hippocampus) to 1.26 (medial occipital cortex). The ratio of the medial occipital cortex to the cerebellum

was significantly higher, and the ratio of the hippocampus to the cerebellum was significantly lower, than the ratios for the other regions ( $P < 0.05$ ). No region showed hemispheric differences in ECD uptake ratios ( $P < 0.05$ ). The mean asymmetry index was small at  $3.6\% \pm 0.8\%$  (range, from 2.2% in the cerebellum to 4.8% in Broca's area). Intersubject variation in regional ECD uptake ratios was also small at  $6.6\% \pm 0.7\%$  for R/CE (range, from 5.4% in the posterior temporal cortex to 7.8% in the anterior cingulate cortex). No sex difference in regional ECD uptake ratios was found.

The relationships between the ECD uptake ratios and age are summarized in Table 4 and shown in Figure 5. R/CE declined significantly with age in the anterior cingulate cortex (2.0% per decade,  $P < 0.0001$ ), striatum (1.6% per decade,  $P = 0.001$ ), hippocampus (1.5% per decade,  $P = 0.0002$ ), superior prefrontal cortex (1.4% per decade,  $P = 0.012$ ), parietal cortex (1.3% per decade,  $P = 0.003$ ), and posterior cingulate cortex (1.0% per decade,  $P = 0.024$ ).

**TABLE 3**  
Quantitative Assessment of ECD Perfusion Patterns: Right-to-Left and Regional Differences

Region	Asymmetry index	R/CE			R/CO		
		Mean	SD	Coefficient variation	Mean	SD	Coefficient variation
SPF	0.026	1.039	0.072	6.976	1.043	0.043	4.122
IPF	0.031	1.059	0.077	7.239	1.063	0.042	3.991
SM	0.033	0.962	0.059	6.090	0.966	0.026	2.741
BC	0.048	1.002	0.063	6.331	1.007	0.038	3.806
OF	0.023	0.865	0.054	6.263	0.869	0.037	4.295
PA	0.031	0.992	0.059	5.977	0.997	0.029	2.868
AT	0.040	0.966	0.059	6.124	0.971	0.044	4.556
PT	0.039	1.067	0.058	5.436	1.072	0.032	3.006
OC	0.040	1.257	0.083	6.565	1.263	0.053	4.188
ST	0.037	1.070	0.068	6.347	1.075	0.055	5.075
TH	0.040	1.117	0.073	6.518	1.123	0.063	5.624
AC		0.791	0.062	7.824	0.795	0.045	5.652
PC		0.864	0.056	6.440	0.869	0.033	3.842
BS		0.880	0.066	7.459	0.884	0.059	6.620
CE	0.022				1.007	0.055	5.468
LT	0.047	0.899	0.058	6.407	N	N	N
HP	0.042	0.709	0.055	7.765	N	N	N

SPF = superior prefrontal cortex; IPF = inferior prefrontal cortex; SM = sensorimotor cortex; BC = Broca's area; OF = orbitofrontal cortex; PA = parietal cortex; AT = anterior temporal cortex; PT = posterior temporal cortex; OC = medial occipital cortex; ST = striatum; TH = thalamus; AC = anterior cingulate cortex; PC = posterior cingulate cortex; BS = brain stem; CE = cerebellum; LT = lateral temporal cortex; N = not determined; HP = medial temporal region including hippocampus.

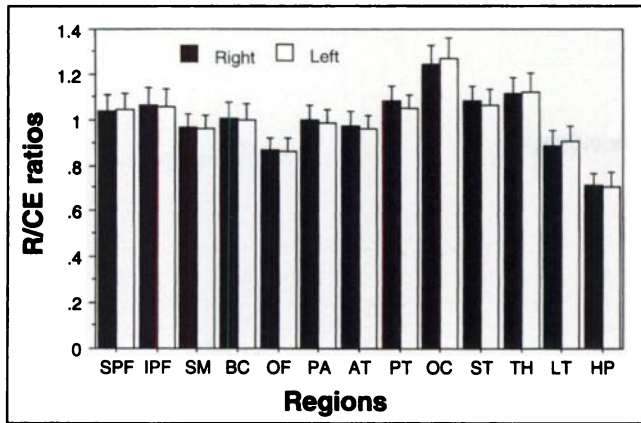


**FIGURE 4.** Significant regional differences were seen in R/CE, ranging from 0.709% in hippocampus (HP) to 1.257% in occipital cortex (OC). Intersubject variability in R/CE in each region was relatively small (mean coefficient variation = 6.6% ± 0.7%). No right-to-left R/CE differences were seen. AT = anterior temporal cortex; BC = Broca's area; HP = medial temporal region including hippocampus; IPF = inferior prefrontal cortex; LT = lateral temporal cortex; OF = orbitofrontal cortex; PA = parietal cortex; PT = posterior temporal cortex; SM = sensorimotor cortex; SPF = superior prefrontal cortex; ST = striatum.

More decreases in the left hemisphere were seen for 10 cerebral cortical regions. In contrast, a significant increase in R/CO with age was observed in the cerebellum (1.0% per decade,  $P = 0.013$ ) and thalamus (1.0% per decade,  $P = 0.028$ ).

## DISCUSSION

### Normal ECD Perfusion Pattern

This study shows that in healthy adults, ECD perfusion patterns vary significantly between regions. The regions of lowest and highest ECD uptake were the medial temporal cortex and the medial occipital cortex, respectively. However, ECD uptake was symmetric between the hemispheres. The intersubject variability of ECD perfusion patterns was relatively small in our quantitative analysis. Visual analysis revealed considerable intersubject variability for the cingulate cortex, with scores ranging from -1 to +1 for all age ranges (Fig. 3). On the other hand, quantitative analysis found relatively little intersubject variability in this region, compared with other regions (R/CE coefficient variation of 7.8% for the anterior cingulate cortex and 6.4% for the posterior cingulate cortex). This discrepancy between the visual and the quantitative findings can be explained by our method of displaying the selected sagittal images of the cingulate cortex for visual analysis. These images were normalized to the pixel containing the highest counts within each image, and this pixel was usually in the occipital cortex. Therefore, visualization of cingulate ECD uptake depended on maximal pixel counts, which varied considerably among subjects.

Loessner et al. (18) reported significant variations in regional cerebral glucose metabolism in their FDG PET study of 120 healthy volunteers. They reported that a frontal eye field was seen on the right in 84.2% of subjects and on

**TABLE 4**  
Relationship Between ECD Uptake Ratios and Age

Region	R/CE			R/CO		
	Slope (r)	Correlation coefficient (R)	P	Slope (r)	Correlation coefficient (R)	P
SPF	-0.0014	-0.359	0.012	-0.0003	-0.145	NS
IPF	-0.0008	-0.208	NS	0.0002	0.096	NS
SM	-0.0006	-0.200	NS	0.0003	0.227	NS
BC	-0.0003	-0.094	NS	0.0007	0.338	0.019
OF	-0.0002	-0.074	NS	0.0006	0.321	0.026
PA	-0.0013	-0.423	0.003	-0.0004	-0.256	NS
AT	-0.0003	-0.101	NS	0.0006	0.278	NS
PT	-0.0004	-0.138	NS	0.0006	0.366	0.011
OC	-0.0012	-0.272	NS	10 <sup>-7</sup>	0.000	NS
ST	-0.0016	-0.450	0.001	-0.0006	-0.206	NS
TH	10 <sup>-5</sup>	-0.003	NS	0.0010	0.318	0.028
AC	-0.0020	-0.611	<0.0001	-0.0012	-0.514	0.0002
PC	-0.0010	-0.325	0.024	-0.0001	-0.078	NS
BS	-0.0005	0.152	NS	0.0003	0.091	NS
CE				0.0010	0.357	0.013
LT	-0.0005	-0.171	NS	N	N	N
HP	-0.0015	-0.507	0.0002	N	N	N

SPF = superior prefrontal cortex; NS = no statistically significant change; IPF = inferior prefrontal cortex; SM = sensorimotor cortex; BC = Broca's area; OF = orbitofrontal cortex; PA = parietal cortex; AT = anterior temporal cortex; PT = posterior temporal cortex; OC = medial occipital cortex; ST = striatum; TH = thalamus; AC = anterior cingulate cortex; PC = posterior cingulate cortex; BS = brain stem; CE = cerebellum; LT = lateral temporal cortex; N = not determined; HP = medial temporal region including hippocampus.

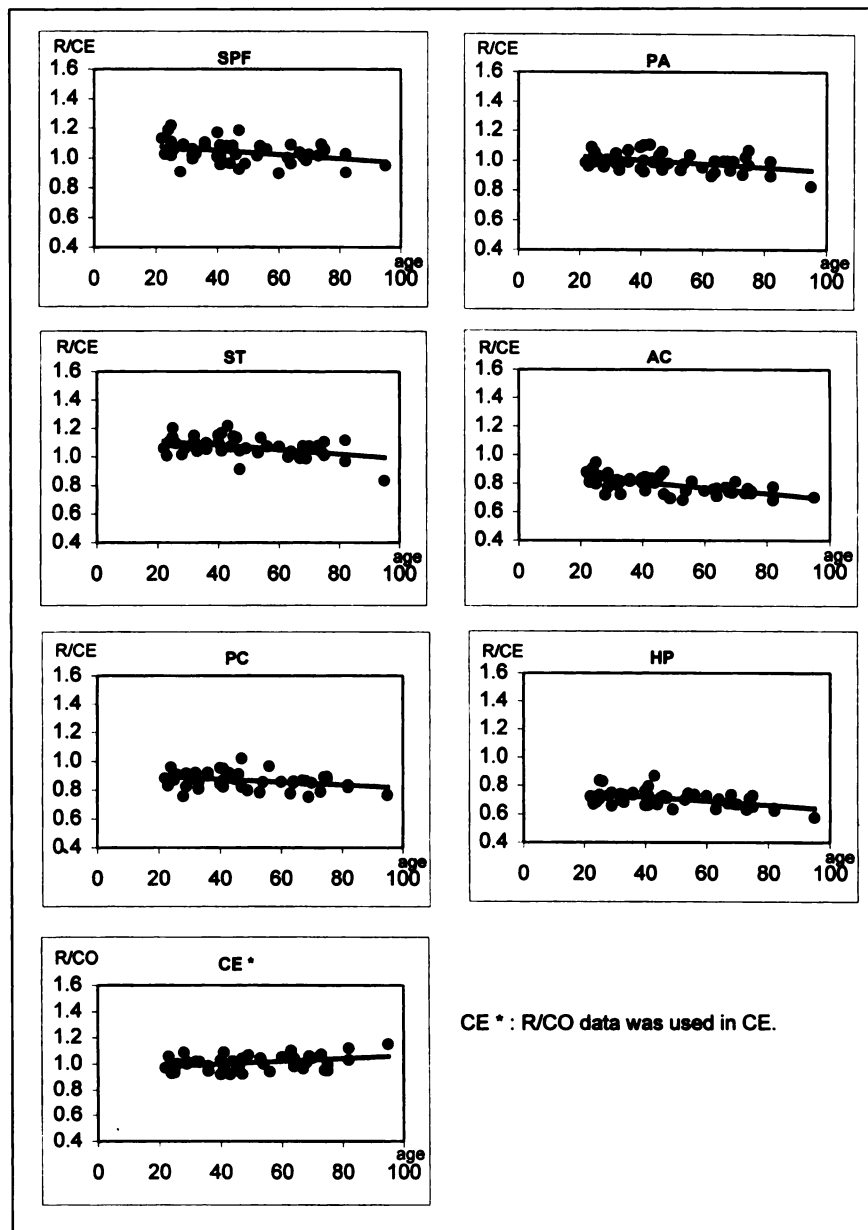


**FIGURE 5.** Relationships between regional ECD uptake ratios (R/CE or R/CO) and age. In 6 regions (superior prefrontal cortex [SPF], parietal cortex [PA], striatum [ST], medial temporal region including hippocampus [HP], anterior cingulate cortex [AC], and posterior cingulate cortex [PC]), R/CE decreased significantly with age by 1.0%–2.0% per decade ( $P < 0.05$ ). In cerebellum (CE), R/CO increased significantly with age by 1.0% per decade ( $P < 0.05$ ).

the left in 76.7% of subjects and that a parieto-occipital junction was seen on the right in 58.3% of subjects and on the left in 46.0% of subjects. Also seen was significant asymmetry of either the temporal or the visual cortex, with ipsilateral decreases in metabolic activity. In our study, a frontal eye field was seen on the right in 47.9% of subjects and on the left in 41.7% of subjects. We saw a parieto-occipital junction on the right in 62.5% of subjects and on the left in 60.4% of subjects. Loessner et al. additionally observed a frontal pole defect on the right in 84.2% of subjects and on the left in 61.7% of subjects, whereas we saw no frontal pole defect. These discrepancies between their findings and ours may be related to major methodologic (PET versus SPECT) and tracer (glucose metabolism versus rCBF) differences. For example, Ishii et al. (32) reported some differences between rCBF and cerebral

metabolic rate for oxygen in healthy volunteers. In addition, all our ECD images were technically adequate, whereas in their FDG PET study 16% of images were rated as technically poor. Further comparisons of metabolism and CBF images in the same subject may be needed to evaluate the functional significance of these variations.

#### Age Effect

Age-related decreases in ECD perfusion pattern were clearly seen in 6 regions, including the anterior and posterior cingulate cortex, striatum, medial temporal region, superior prefrontal cortex, and parietal cortex. These areas were reported to be highly affected by aging in other rCBF studies using PET (22) or  $^{99m}\text{Tc}$ -D,L-hexamethyl propyleneamine oxime SPECT (13,33). To obtain adequate counts in the cingulate ROIs, we added 3 continuous slices, including the

midsagittal slice. This step may have caused an overestimation of age-related decreases in ECD uptake in the cingulate cortex because of the partial-volume effect from underlying age-related cortical atrophy. However, the decline of ECD uptake ratios was smaller in the posterior cingulate cortex than in the anterior cingulate cortex. Minoshima et al. (34) suggested that the posterior cingulate cortex is functionally important in learning and memory, and those regions are affected very early in Alzheimer's disease as shown by FDG PET. Our quantitative ECD technique may be helpful for detecting findings similar to those of Minoshima et al. in the posterior cingulate cortex.

Although visual assessment of the medial temporal region is difficult because of its inherently low ECD uptake, we were able to show a significant age-related decrease in ECD uptake in this region by quantitative analysis. Other investigators also found low ECD uptake on visual analysis of the medial temporal cortex (26–28). They suggested that low ECD uptake in the hippocampus may result in a false-negative visual interpretation of hippocampal abnormalities in patients with dementia or epilepsy. Therefore, quantitative analysis would be better suited for evaluating hippocampal abnormalities on ECD images.

A previously reported ECD perfusion pattern in children differs from our results for adults. Schiepers et al. (35) reported that the highest ECD uptake was seen in the striatum of children aged 1.3–2.3 y, although the medial occipital cortex became the highest after the age of 4.8 y. On the other hand, Barthel et al. (36) reported that the medial occipital cortex had the same ECD uptake as the striatum in children aged 4–15 y. Using  $^{133}\text{Xe}$  or  $^{123}\text{I}$ -iodoamphetamine, rCBF SPECT studies revealed that the rCBF distribution pattern changes during brain maturation in children (37–38) and that rCBF increases with age faster in the striatum than in other cerebral regions. In addition to such developmental changes in rCBF distribution, developmental changes in the retention mechanism of ECD may exist, possibly explaining the dramatic differences in ECD perfusion patterns between children and adults.

A significant increase in ECD uptake in the cerebellum relative to the cerebral cortex was noted for R/CO data, although this finding was not shown either in quantitative rCBF studies using PET (21) or in studies using SPECT (33). Our finding of an increased cerebellum-to-cerebral cortex ECD uptake ratio with age is consistent with the findings of an FDG PET study by Loessner et al. (18) in which relative cerebellar metabolic activity increased with age because of a greater decline in cerebral metabolic activity compared with cerebellar metabolic activity.

## CONCLUSION

ECD brain SPECT images in adults show a significant regional variation in ECD uptake. A frontal eye field and parieto-occipital junction are seen as a high incidence of focally increased ECD uptake. A small but significant age-related change is seen in some regions. However,

hemispheric asymmetry and intersubject variability of ECD perfusion pattern are relatively small in adults. Recognition of these normal perfusion patterns is important in interpreting clinical ECD SPECT studies.

## ACKNOWLEDGMENTS

This study was supported by DuPont Merck Pharmaceutical Company, Montreal, Canada; a grant from the Medical Research Council of Canada (HT-13367); an Acenberg award from Rotman Research Institute, Toronto, Canada; and the Saul A. Silverman Family Foundation, Toronto, Canada, as a Canada-International Scientific Exchange Program project.

## REFERENCES

- Walovitch RC, Francheschi M, Picard M, et al. Metabolism of  $^{99\text{m}}\text{Tc}$ -L,L-ethyl cysteinyl dimer in healthy volunteers. *Neuropharmacology*. 1991;30:283–292.
- Walovitch RC, Cheesman EH, Maheu LJ, Hall KM. Studies of the retention mechanism of the brain perfusion imaging agent  $^{99\text{m}}\text{Tc}$ -bicisate ( $^{99\text{m}}\text{Tc}$ -ECD). *J Cereb Blood Flow Metab*. 1994;14(suppl 1):S4–S11.
- Walovitch RC, Hill TC, Garrity ST, et al. Characterization of technetium- $^{99\text{m}}$ -L,L-ECD for brain perfusion imaging. Part 1. Pharmacology of technetium- $^{99\text{m}}$ -ECD in nonhuman primates. *J Nucl Med*. 1989;30:1892–1901.
- Leveille J, Demonceau G, Roo MD, et al. Characterization of technetium- $^{99\text{m}}$ -L,L-ECD for brain perfusion imaging. Part 2. Biodistribution and brain imaging in humans. *J Nucl Med*. 1989;30:1902–1910.
- Vallabhajosula S, Zimmerman RE, Picard M, et al. Technetium- $^{99\text{m}}$ -ECD: a new brain imaging agent: in vivo kinetics and biodistribution studies in normal human subjects. *J Nucl Med*. 1989;30:599–604.
- Leveille J, Demonceau G, Walovitch RC. Intrasubject comparison between technetium- $^{99\text{m}}$ -ECD and technetium- $^{99\text{m}}$  HMPAO in healthy human subjects. *J Nucl Med*. 1992;33:480–484.
- Lassen NA, Sperling B.  $^{99\text{m}}\text{Tc}$ -bicisate reliably images CBF in chronic brain diseases but fails to show reflow hyperemia in subacute stroke: report of a multicenter trial of 105 cases comparing  $^{133}\text{Xe}$  and  $^{99\text{m}}\text{Tc}$ -bicisate (ECD, Neurolite) measured by SPECT on same day. *J Cereb Blood Flow Metab*. 1994;14(suppl 1):S44–S48.
- Brass LM, Walovitch RC, Joseph JL, et al. The role of single photon emission computed tomography brain imaging with  $^{99\text{m}}\text{Tc}$ -bicisate in the localization and definition of mechanism of ischemic stroke. *J Cereb Blood Flow Metab*. 1994;14(suppl 1):S91–S98.
- Nakagawara J, Nakamura J, Takeda R, et al. Assessment of postischemic reperfusion and diamox activation test in stroke using  $^{99\text{m}}\text{Tc}$ -ECD SPECT. *J Cereb Blood Flow Metab*. 1994;14(suppl 1):S49–S57.
- Shishido F, Umemura K, Murakami M, et al. Cerebral uptake of  $^{99\text{m}}\text{Tc}$ -bicisate in patients with cerebrovascular disease in comparison with CBF and CMRO<sub>2</sub> measured by positron emission tomography. *J Cereb Blood Flow Metab*. 1994;14(suppl 1):S66–S75.
- Grunwald F, Menzel C, Pavics L, et al. Ictal and interictal brain SPECT imaging in epilepsy using technetium- $^{99\text{m}}$ -ECD. *J Nucl Med*. 1994;35:1896–1901.
- Menzel C, Steidele S, Grunwald F, et al. Evaluation of technetium- $^{99\text{m}}$ -ECD in childhood epilepsy. *J Nucl Med*. 1996;37:1106–1112.
- Waldemar G, Walovitch RC, Andersen AR, et al.  $^{99\text{m}}\text{Tc}$ -bicisate (Neurolite) SPECT brain imaging and cognitive impairment in dementia of the Alzheimer type: a blinded read of image sets from a multicenter SPECT trial. *J Cereb Blood Flow Metab*. 1994;14(suppl 1):S99–S105.
- van Dyck CH, Lin CH, Smith EO, et al. Comparison of technetium- $^{99\text{m}}$ -HMPAO and technetium- $^{99\text{m}}$ -ECD cerebral SPECT images in Alzheimer's disease. *J Nucl Med*. 1996;37:1749–1755.
- Bartenstein P, Minoshima S, Hirsch C, et al. Quantitative assessment of cerebral blood flow in patients with Alzheimer's disease by SPECT. *J Nucl Med*. 1997;38:1095–1101.
- Miletich RS, Quarantelli M, Chiro GD. Regional cerebral blood flow imaging with  $^{99\text{m}}\text{Tc}$ -bicisate SPECT in asymmetric Parkinson's disease: studies with and without chronic drug therapy. *J Cereb Blood Flow Metab*. 1994;14(suppl 1):S106–S114.
- Deutsch G, Mountz JM, Katholi CR, et al. Regional stability of cerebral blood flow measured by repeated technetium- $^{99\text{m}}$ -HMPAO SPECT: implications for the study of state-dependent change. *J Nucl Med*. 1997;38:6–13.

18. Loessner A, Alavi A, Lewandrowski KU, et al. Regional cerebral function determined by FDG-PET in healthy volunteers: normal patterns and changes with age. *J Nucl Med.* 1995;36:1141-1149.
19. Sokoloff L. Relationships among local functional activity, energy metabolism, and blood flow in the central nervous system. *Fed Proc.* 1981;40:2311-2316.
20. Pantano P, Baron JC, Lebrun-Grandie P, et al. Regional cerebral blood flow and oxygen consumption in human aging. *Stroke.* 1984;15:635-641.
21. Yamaguchi T, Kanno I, Uemura K, et al. Reduction in regional cerebral metabolic rate of oxygen during human aging. *Stroke.* 1986;17:1220-1228.
22. Martin AJ, Friston KJ, Colebatch JG, et al. Decreases in regional cerebral blood flow with normal aging. *J Cereb Blood Metab.* 1991;11:684-689.
23. Yonekura Y, Tsuchida T, Sadato N, et al. Brain perfusion SPECT with <sup>99m</sup>Tc-bicisate: comparison with PET measurement and linearization based on permeability-surface area product model. *J Cereb Blood Metab.* 1994;14(suppl 1):S58-S65.
24. Tsuchida T, Nishizawa S, Yonekura Y, et al. SPECT images of technetium-99m-ethyl cysteinyl dimer in cerebrovascular diseases: comparison with other cerebral perfusion tracers and PET. *J Nucl Med.* 1994;35:27-31.
25. Ichise M, Golan H, Ballinger JR, et al. Regional differences in technetium-99m-ECD clearance on brain SPECT in healthy subjects. *J Nucl Med.* 1997;38:1253-1260.
26. Matsumura K, Watanabe Y, Aoki S, et al. Evaluation of regional cerebral blood flow in hippocampus by <sup>99m</sup>Tc-ECD SPECT: comparison with <sup>123</sup>I-IMP SPECT. *Kaku Igaku.* 1996;33:1021-1026.
27. Oku N, Matsumoto M, Hashikawa K, et al. Intra-individual differences between technetium-99m-HMPAO and technetium-99m-ECD in the normal medial temporal lobe. *J Nucl Med.* 1997;38:1109-1111.
28. Koyama M, Kawashima R, Ito H, et al. SPECT imaging of normal subjects with technetium-99m-HMPAO and technetium-99m-ECD. *J Nucl Med.* 1997;38:587-592.
29. Hugo D, Rousseaux M, Leys D, et al. Regional cerebral blood flow imaging: a quantitative comparison of <sup>99m</sup>Tc-bicisate with <sup>133</sup>Xe using single photon emission computed tomography. *J Cereb Blood Metab.* 1994;14(suppl 1):508-521.
30. Tsao J, Stundzia A, Ichise M. Fully automated establishment of stereotaxic image orientation in six degrees of freedom for technetium-99m-ECD brain SPECT. *J Nucl Med.* 1998;39:503-508.
31. Talairach J, Tournoux P, Rayport M. *Co-Planar Stereotaxic Atlas of the Human Brain: Three-Dimensional Proportional System—An Approach to Cerebral Imaging.* New York, NY: Thieme;1988;1-122.
32. Ishii K, Sasaki M, Kitagaki H, et al. Regional difference in cerebral blood flow and oxidative metabolism in human cortex. *J Nucl Med.* 1996;37:1086-1088.
33. Matsuda H, Tsuji S, Shuke N, et al. Noninvasive measurements of regional cerebral blood flow using technetium-99m hexamethylpropylene amine oxime. *Eur J Nucl Med.* 1993;20:391-401.
34. Minoshima S, Giordani B, Berent S, et al. Metabolic reduction in the posterior cingulate cortex in very early Alzheimer's disease. *Ann Neurol.* 1997;42:85-94.
35. Schiepers C, Verbruggen A, Casaer P, et al. Normal brain perfusion pattern of technetium-99m-ethylcysteinyl dimer in children. *J Nucl Med.* 1997;38:1115-1120.
36. Barthel H, Wiener M, Dannenberg C, et al. Age-specific cerebral perfusion in 4- to 15-year-old children: a high-resolution brain SPET study using <sup>99m</sup>Tc-ECD. *Eur J Nucl Med.* 1997;24:1245-1252.
37. Chiron C, Raynaud C, Maziere B, et al. Changes in regional cerebral blood flow during brain maturation in children and adolescents. *J Nucl Med.* 1992;33:696-703.
38. Tokumaru AM, Barkovich J, O'uchi T, et al. The evaluation of cerebral blood flow in the developing brain: evaluation with iodine-123 iodoamphetamine SPECT and correlation with MR imaging. *Am J Neuroradiol.* 1999;20:845-852.